# Superenantioselective Chiral Surface Explosions

Andrew J. Gellman,*,[†,‡] Ye Huang,[†] Xu Feng,[†] Vladimir V. Pushkarev,[†] Brian Holsclaw,[†] and Bharat S. Mhatre[†]

[†]Department of Chemical Engineering, Carnegie Mellon University, 5000 Forbes Avenue, Pittsburgh, Pennsylvania 15213, United States

[‡]National Energy Technology Laboratory, US Department of Energy, P.O. Box 10940, Pittsburgh, Pennyslvania 15236, United States

S *Supporting Information*

ABSTRACT: Chiral inorganic materials predated life on Earth, and their enantiospecific surface chemistry may have played a role in the origins of biomolecular homochirality. However, enantiospecific differences in the interaction energies of chiral molecules with chiral surfaces are small and typically lead to modest enantioselectivities in adsorption, catalysis, and chemistry on chiral surfaces. To yield high enantioselectivities, small energy differences must be amplified by reaction mechanisms such as autocatalytic surface explosions which have nonlinear kinetics. Herein, we report the first observations of superenantiospecificity resulting from an autocatalytic surface explosion reaction of a chiral molecule on a naturally chiral surface. R,R- and S,S-tartaric acid decompose via a

Cu(643)^S Cu(643)^R

vacancy-mediated surface explosion mechanism on Cu single crystal surfaces. When coupled with surface chirality, this leads to decomposition rates that exhibit extraordinarily high enantiospecificity. On the enantiomorphs of naturally chiral Cu(643)$^{R\&S}$, Cu(17,5,1)$^{R\&S}$, Cu(531)$^{R\&S}$ and Cu(651)$^{R\&S}$ single crystal surfaces, R,R- and S,S-tartaric acid exhibit enantiospecific decomposition rates that differ by as much as 2 orders of magnitude, despite the fact that the effective rates constants for decomposition differ by less than a factor of 2.
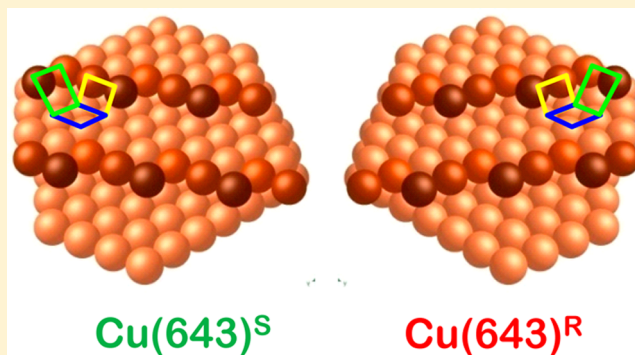
INTRODUCTION

Homochirality is one of the hallmarks of the biomolecular building blocks of life on Earth and the mechanism of its origin has stimulated significant debate.[1] Naturally chiral minerals such as quartz predate chiral organic compounds on Earth, and it has been suggested that enantioselective chemistry on the chiral surfaces of such inorganic materials played a role in the origins of biomolecular homochirality.[2,3] Today, chiral surfaces can be used to impart enantioselectivity to important chemical processes such as adsorption, crystallization, and catalysis. One of the greatest challenges to the development of highly enantioselective surface chemistry is rooted in the fact that the enantiospecific interaction energetics of chiral molecules with chiral surfaces differ by only a few kJ/mol, resulting in weakly enantiospecific rate constants. In principle, weakly enantiospecific rate constants can be amplified into highly enantiospecific reaction rates by processes such as autocatalysis which have nonlinear reaction kinetics. In this article, we report the first example of such a highly enantiospecific, nonlinear process coupling autocatalysis with surface chirality; the autocatalytic, vacancy-mediated explosive decomposition of R,R- and S,S-tartaric acid on the naturally chiral Cu(643)$^{R\&S}$, Cu(17,5,1)$^{R\&S}$, Cu(531)$^{R\&S}$ and Cu(651)$^{R\&S}$ single crystal surfaces. Tartaric acid decomposition on chiral Cu surfaces can exhibit enantiospecific rates that differ by almost 2 orders of

magnitude. Such enantiospecific autocatalytic processes may be the key to development of highly enantioselective surface chemistry and catalysis. They may also provide insight into the types of chemical processes that may have led to the homochiral biochemistry of life on Earth.

One of the central questions in the debate over the origins of biomolecular homochirality is whether there is a chiral bias in Nature that determined the chirality of naturally occurring biomolecules or whether a stochastic fluctuation in the enantiomeric excess of an early chiral species was amplified to cause that enantiomer to dominate.[1] Chiral amplification can arise from processes in which a chiral catalytic species, R, transforms a prochiral reagent, A, into another molecule of catalyst while preserving its chirality.

$$A \xrightarrow{R} R$$

Moreover, if one enantiomer actively suppresses the formation of the other, such an autocatalytic process would lead to a net enantiomeric excess from an achiral reactant. The only known example of such enantioselective autocatalysis is the Soai reaction in which R- or S-pyrimidyl alkanol catalyzes the enantioselective addition of diisopropylzinc to pyrimidine-5-
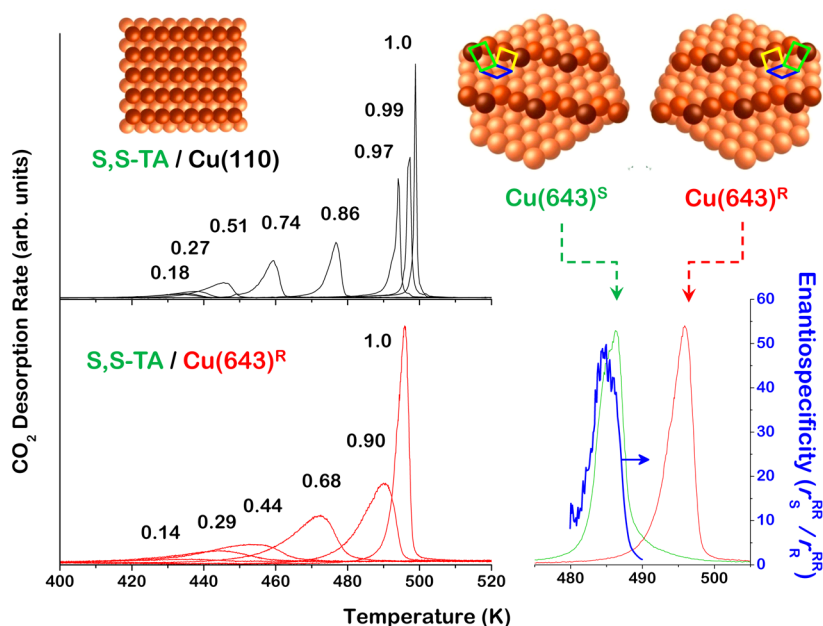
Figure 1. Rate of CO_2 desorption during temperature programmed reaction (TPR) of S,S-TA/Cu(110) and S,S-TA/Cu(643)$^{R\&S}$. (Upper left) TPR for initial coverages of $\theta_0^{SS\text{-}TA} = 0.18 \rightarrow 1.0$ ML on Cu(110).[7] The initial coverages are marked on the figure. The peak shift from $T_p = 432 \rightarrow 499$ K and the extraordinarily narrow peak width of $\Delta T_p < 1$ K at $\theta_0^{SS\text{-}TA} = 1$ ML are signatures of the vacancy-mediated, explosive decomposition mechanism. (Lower left) TPR of S,S-TA/Cu(643)^R (structure shown in upper right) for initial coverages of $\theta_0^{SS\text{-}TA} = 0.14 \rightarrow 1.0$ ML (marked on figure). These also show the signature characteristics of an explosive decomposition mechanism. (Upper right) The enantiomorphic structures of the chiral Cu(643)$^{R\&S}$ surfaces. The chirality is dictated by the sense of rotation among the blue (111), yellow (100), and green (110) microfacets. (Lower right) The TPR of S,S-TA/Cu(643)$^{R\&S}$ reveals superenantiospecific decomposition kinetics. The peak reaction temperatures are $T_p^{SS/R} = 496$ K (red curve) and $T_p^{SS/S} = 486$ K (green curve). The ratio of the rates (blue curve) reaches a maximum of $r_S^{SS}/r_R^{SS} = 50$ at $T = 485$ K. (Heating rate = 1 K/s, $m/q = 44$ amu).

carbaldehyde to yield R- or S-pyrimidyl alkanol while preserving chirality.[4] Seeding a mixture of diisopropylzinc and pyrimidine-5-carbaldehyde with d- or l-quartz enantiospecifically biases the initial production of pyrimidyl alkanol, and the subsequent homogeneous phase autocatalysis results in a large enantiomeric excess of S- or R-pyrimidyl alkanol.[5]

Herein, we report the discovery and study of a highly enantiospecific, autocatalytic surface reaction, the vacancy-mediated explosive decomposition of R,R- or S,S-tartaric acid (TA) on naturally chiral Cu single crystal surfaces. This heterogeneous process bears some similarity to the homogeneous Soai reaction in the sense that it is autocatalytic; on a chiral surface an empty chiral adsorption site or vacancy catalyzes the decomposition of TA to yield two vacancies of the same chirality. As a direct consequence of its autocatalytic nature, the decomposition of TA on chiral Cu surfaces is highly enantiospecific. Despite that the enantiospecific differences in the reaction energetics are only a few kJ/mol, the nonlinear explosion kinetics lead to enantiospecific rates that differ by almost 2 orders of magnitude. A distinction between the Soai reaction and this autocatalytic surface reaction is that the chirality of the empty site is predetermined by the crystallographic orientation of the surface. The branching step in this autocatalytic explosion mechanism would be represented by

$$A*_R \xrightarrow{\;*_R\;} P_{(g)} + *_R$$
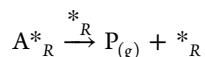
where $*_R$ denotes a surface reaction site of R chirality and A is the adsorbed reactant that yields the gas phase product $P_{(g)}$. This understanding offers an opportunity to design heterogeneous processes on chiral surfaces that are highly enantiose-lective and circumvent the limitations of weakly enantiospecific reaction energetics.

■ EXPERIMENTAL METHODS

Experiments were performed in several ultrahigh vacuum chambers. Each was equipped with an xyz-φ sample manipulator capable of moving the Cu single crystal sample within the chamber and allowing heating and cooling in the temperature range 80−1000 K. The chambers were all equipped with low energy electron diffraction (LEED) optics, Ar$^+$ ion sources for cleaning the surfaces of Cu single crystal samples, glass Knudsen cells for temperature controlled sublimation of TA, and quadrupole mass spectrometers for measurement of CO_2 desorption rates during TA decomposition.

Cu(hkl)$^{R\&S}$ single crystals polished on both sides were purchased from Monocrystals Inc. Note that one side of these crystals exposes the Cu(hkl)^R surface while the other exposes the Cu(hkl)^S surface. The absolute chirality can be determined using either LEED or X-ray diffraction.[6] The Cu(hkl)$^{R\&S}$ surfaces were cleaned in ultrahigh vacuum by cycles of Ar$^+$ ion sputtering followed by annealing at temperatures in the range 800−1000 K. X-ray photoemission spectroscopy was used to develop procedures that yielded clean surfaces. TA was then deposited onto the surfaces from glass sublimation sources heated to temperatures in the range 350−370 K. The sources were equipped with shutters that were used to control the time of surface exposure to the TA vapor. TA was adsorbed with the Cu(hkl) surfaces at a temperature of 405 K in order to allow saturation of the surface without adsorption of a multilayer film.

R,R-TA and S,S-TA were purchased from Aldrich Chemical Co. and treated by extended sublimation in vacuum to remove any low vapor pressure contaminants prior to use.

Temperature programmed reaction of the TA/Cu(hkl) was conducted by positioning the sample in front of the aperture to the mass spectrometer and then heating the surface at a constant rate of 1 K/s while monitoring the mass spectrometer signal at $m/q = 44$ amu. In the isothermal experiments the sample was heated at a rate of 1 K/s

to the desired temperature and then held at constant temperature. The overshoot in the temperature was ~1 K and the settling time under feedback control was ~10 s.[7]

RESULTS

Although it is counterintuitive that the surfaces of achiral materials such as metals can be chiral, it is more common than not, in the sense that any surface with an atomic structure that lacks mirror plane symmetry will be chiral. Cleaving the bulk structure of a metal along a low symmetry direction exposes a chiral surface.[8,9] All of the surfaces represented by points in the interior of the stereographic triangle used to enumerate crystal planes are chiral. Only the surfaces represented by the vertices and the points along the edges of the stereographic triangle have mirror symmetry and are achiral. Such surfaces have ideal structures based on the projections of the three low Miller index microfacets out of the surface, as shown for the $Cu(643)^{R\&S}$ surfaces in the upper right panel of Figure 1. The (111), (100), and (110) microfacets forming the terrace, step, and kink are indicated in blue, yellow, and green, respectively, and the chirality of the surface is dictated by the sense of rotation among the three.[10,11] The combinations of low Miller index microfacets forming the terrace, step, and kink on the four chiral surface orientations used in this work are listed in Table S1 of the Supporting Information. The two mirror images of $Cu(643)^{R\&S}$ are clearly nonsuperimposable and, therefore, chiral. The real structures of such surfaces are complicated by phenomena such as atomic scale thermal roughening of the kinked step edges; however, scanning tunneling microscopy images of $Cu(643)^{R}$ and $Cu(531)^{S}$ surfaces show that their chirality is preserved.[12,13] The distribution of local step lengths and terrace widths resulting from thermal roughening of chiral surfaces is reproducible. The critical metric of the reproducibility of the chiral surface structures is the demonstration of diastereomerism in their interactions with chiral adsorbates. If the properties measured for the R- or S-adsorbate on the R- or S-surface have the relationship $P_R^R = P_S^S \neq P_R^S = P_S^R$, then the enantiospecific differences must arise only from the enantiospecific differences in the surface structure. Enantiospecific interaction of chiral molecules with naturally chiral metal surfaces has been demonstrated by various means in various laboratories; however, the enantiospecificities of adsorption or surface reaction energetics are limited to a few kJ/mol and the resulting enantioselectivities are low.[6,10,14−22] Circumventing the limitations of weakly enantiospecific reaction energetics on chiral surfaces, in order to develop processes that are highly enantioselective, is a challenge to the development of enantioselective heterogeneous catalysts and adsorbents.

Since its first use by Pasteur in the form of sodium ammonium tartrate in his seminal discovery of molecular chirality,[23] tartaric acid has held a central place in the study of enantiospecific chemistry, and more recently in surface chemistry. The surface chemistry of TA on the achiral Cu(110) surface has been elucidated over the past decade.[7,24−26] At low coverages and temperatures in the range of 300−400 K, R,R- and S,S-TA adsorb as a doubly deprotonated species ($-O_2CCH(OH)CH(OH)CO_2-$) and form enantiomorphous (9,0; ±2,1) ordered overlayers. At an absolute coverage of [TA] = 0.25 per Cu atom, both enantiomers are singly deprotonated ($-O_2CCH(OH)CH-(OH)CO_2H$) and adsorb in a c(4 × 2) lattice. At saturation

coverage of [TA] = 0.278 per Cu, the singly deprotonated form is adsorbed in enantiomorphous (4,1; ±2,4) lattices.

During heating adsorbed TA decomposes in the temperature range of 430−500 K to yield CO_2, H_2, and H_2O plus several small hydrocarbons.[7,25,26] The rate of CO_2 desorption is readily measured using mass spectrometry. It is limited by the rate of TA decomposition on the surface, and thus the CO_2 desorption rate serves as a measure of the surface reaction rate. From the perspective of this report, the important feature of the surface chemistry of TA/Cu(110) is that during heating to greater than 400 K its decomposition proceeds via a vacancy-mediated, autocatalytic surface explosion.[7,25,26] In a vacancy-mediated surface explosion, an adsorbed species, A*, requires an adjacent vacant site, *, in order to decompose to yield gas phase products, $A* \overset{*}{\rightarrow} P_{(g)} + *$. The process is autocatalytic in the sense that one vacancy begets two vacancies; two beget four and so on, leading to an exponential increase in the vacancy concentration. This surface reaction mechanism is called an explosion by analogy with the radical branching mechanism of a gas phase radical explosion. Because the reaction rate depends on the coverages of both adsorbate and vacancies, the rate law is nonlinear and of the form $r = k\theta(1 - \theta)$ where k is the effective rate constant, θ is the fractional coverage of adsorbate, and $(1 - \theta)$ is the fractional coverage of vacancies on the surface. The upper left panel of Figure 1 shows the temperature programmed decomposition of S,S-TA on Cu(110) to yield CO_2 desorption.[7] The reaction rate is measured for initial fractional coverages of $\theta_0^{TA} = 0.18 \rightarrow 1.0$ by monitoring the rate of CO_2 desorption as a function of temperature during heating at 1 K/s. One signature feature of a surface explosion is the dramatic increase in peak desorption temperature, T_p, with increasing θ_0^{TA}. The second is that for $\theta_0^{TA} \approx 1$ an initiation process leads to initial vacancy formation after which the autocatalytic explosion in vacancy concentration leads to reaction completion over a very narrow temperature range, $\Delta T_p < 1$ K in the case of S,S-TA/Cu(110).

Many discussions of surface explosion reactions assume that initiation of the reaction occurs at defects in the surface.[7,27,28] As such, it is not clear that TA decomposition on chiral surfaces such as $Cu(643)^{R\&S}$ would occur via an explosion mechanism because the density of kink defects on the surface is roughly equivalent to the absolute TA coverage. Nonetheless, as demonstrated in the lower left panel of Figure 1, the temperature programmed decomposition of S,S-TA/Cu(643)^R exhibits the two signatures of an explosive decomposition mechanism. The peak temperature shifts with increasing initial S,S-TA coverage from 430 K at low coverage to 496 K at $\theta_0^{TA} = 1.0$ and the peak width drops to $\Delta T_p = 3.5$ K. The peak widths on $Cu(643)^R$ are greater than on Cu(110); this may arise from the heterogeneity in local surface structure caused by thermal roughening.[12] The key observation of this work is illustrated in the lower right panel of Figure 1 which shows the peaks for decomposition of S,S-TA at $\theta_0^{TA} = 1.0$ on the $Cu(643)^R$ and $Cu(643)^S$ surfaces. The TPR spectra in red are measures of the enantiospecific rates of decomposition of S,S-TA on the $Cu(643)^S$ surface, r_S^{SS}, and on the $Cu(643)^R$ surface, r_R^{SS}. The blue curve is the ratio of the two and reveals highly enantiospecific decomposition rates. The enantiospecificity reaches a value of $r_S^{SS}/r_R^{SS} = 50$ at 485 K, over an order of magnitude higher than any other enantiospecificity observed on a naturally chiral surface.[6,10,14,15,17−22,29] The highest of these previously measured enantioselectivities have been observed for the electrooxidation of glucose on $Pt(531)^{R\&S}$ electrodes,[10] the
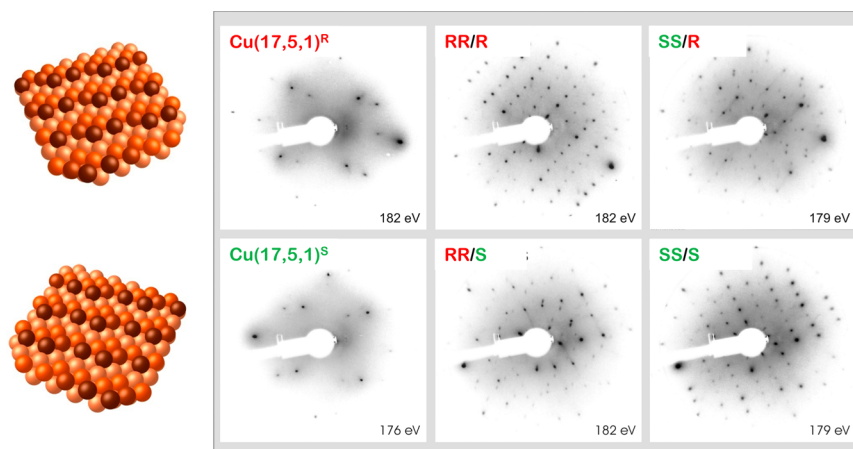
Figure 2. LEED patterns for the clean $Cu(17,5,1)^{R\&S}$ surfaces and for saturated monolayers of R,R- and S,S-TA on $Cu(17,5,1)^{R\&S}$. The stepped structure of the clean $Cu(17,5,1)^{R\&S}$ surfaces is revealed by the splitting of the diffraction spots and their chirality is revealed by the mirror reflection of the splitting direction through the horizontal. The saturated monolayers of R,R-TA/$Cu(17,5,1)^R$ (denoted RR/R) and SS/S form overlayer lattices with the same periodicity (1×1) as the substrate surfaces, again related by mirror symmetry through the vertical. The LEED patterns for SS/R and RR/S are also related by mirror symmetry through the vertical but are unrelated to those formed by RR/R and SS/S. The overlayer lattices for SS/R and RR/S are complex, have not been assigned, and probably consist of multiple domains. Nonetheless, the set of LEED patterns reveal the diastereomeric relationship between the overlayer lattices formed by R,R- and S,S-TA at saturation coverage on the $Cu(17,5,1)^{R\&S}$ surfaces.
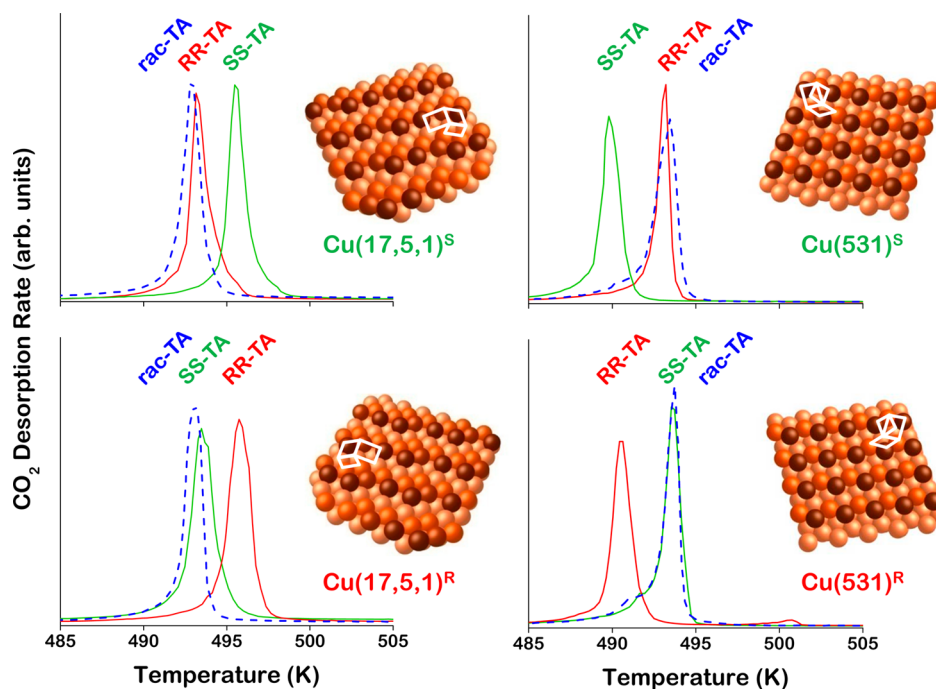

Figure 3. TPR of R,R-TA, S,S-TA, and rac-TA on $Cu(17,5,1)^{R\&S}$ and $Cu(531)^{R\&S}$ surfaces. (Left panel) TPR of R,R- and S,S-TA on $Cu(17,5,1)^{R\&S}$ reveals high enantiospecificity and diastereomerism: $T_p^{RR/S} = T_p^{SS/R} < T_p^{RR/R} = T_p^{SS/S}$. Decomposition of the rac-TA occurs at the same temperature on both surfaces, $T_p^{rac/S} = T_p^{rac/R} = T_p^{SS/R}$. (Right panel) TPR of R,R- and S,S-TA on $Cu(531)^{R\&S}$ reveals high enantiospecificity and diastereomerism; however, the order of stability is reversed from that on $Cu(17,5,1)^{R\&S}$: $T_p^{RR/S} = T_p^{SS/R} > T_p^{RR/R} = T_p^{SS/S}$. Decomposition of the rac-TA occurs at the same temperature on both surfaces but at the temperature of the more stable adsorbate−surface combination, $T_p^{rac/S} = T_p^{rac/R} = T_p^{SS/R}$.

electron induced dissociation of methyl lactate on $Cu(643)^R$,[20] and the desorption of lysine from the $Cu(3,1,17)^{R\&S}$ surfaces.[22] The enantiospecificities of reaction rates observed in these systems has been in the range of 2−4, far less than the enantiospecificity observed in this work for the autocatalytic decomposition of TA on naturally chiral Cu surfaces.

The extraordinarily high enantiospecificity of explosive TA decomposition appears to be general to chiral $Cu(hkl)^{R\&S}$ surfaces and in this work has been observed on the $Cu(643)^{R\&S}$, $Cu(17,5,1)^{R\&S}$, $Cu(651)^{R\&S}$ and $Cu(531)^{R\&S}$

surfaces. All of these are naturally chiral and have been selected for the variety of their structures; the $Cu(643)^{R\&S}$, $Cu(17,5,1)^{R\&S}$ and $Cu(651)^{R\&S}$ surfaces have terraces formed by microfacets of the three different low Miller index planes: (111), (100), and (110), respectively (see Table S1 in the Supporting Information section). These terraces are separated by monatomic, kinked step edges. The $Cu(531)^{R\&S}$ surfaces are the 'most' chiral surfaces in the sense that they have the highest possible chiral kink density. The three microfacets are all one
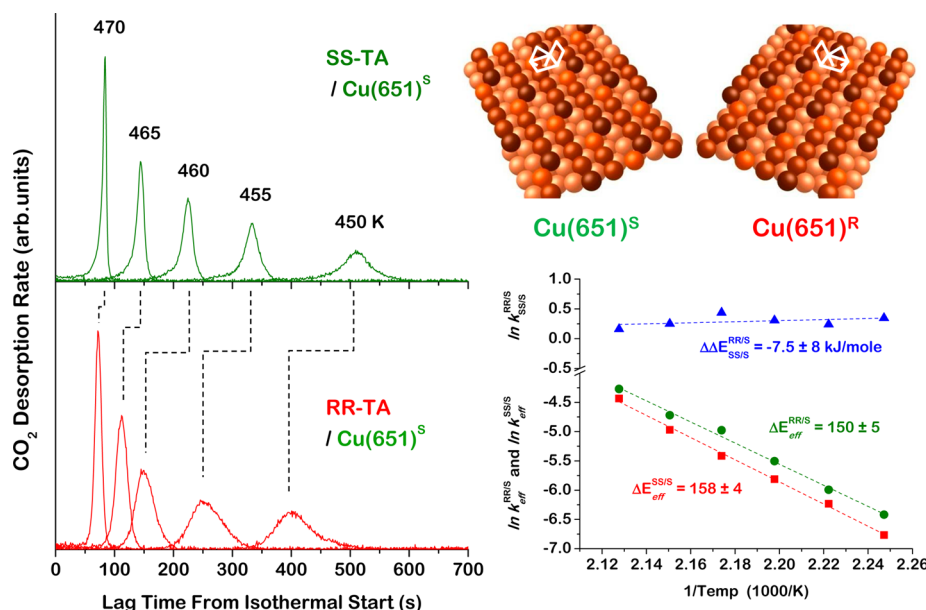
Figure 4. (Left panel) Isothermal decomposition of R,R-TA and S,S-TA on $Cu(651)^S$ (structure in upper right panel) with $\theta_0^{RR\text{-}TA} = \theta_0^{SS\text{-}TA} = 1$ ML and temperatures in the range of 450−470 K. The explosive decomposition is characterized by an initiation period followed by an autocatalytic increase in reaction rate. Enantiospecificity is manifested by the dependence of the peak reaction time, t_p, on the relative chirality of the R,R- and S,S- TA and the $Cu(651)^S$ surface. (Lower right) Plot of $\ln(k_{eff})$ versus T^{-1}, where $k_{eff} = t_p^{-1} = (1/2)(k_i k_e)^{1/2}$. The slopes yield the effective barriers for TA decomposition, $\Delta E_{eff} = (1/2)(\Delta E_i + \Delta E_e)$, but the enantiospecific difference is not significantly different from zero.

unit cell wide and thus, cannot be categorized as forming terrace, steps or kinks.[6,13]

Adsorption of R,R- and S,S-TA on the $Cu(17,5,1)^{R\&S}$ surfaces yielded adsorbed layers with long-range periodic order that was detectable using low energy electron diffraction (LEED) as illustrated in Figure 2. The splitting in the LEED spots from the clean $Cu(17,5,1)^{R\&S}$ surfaces is characteristic of electron diffraction from stepped surfaces. The fact that the splitting directions are mirrored through the vertical in the patterns from the clean surfaces is indicative of their chirality and the enantiomorphous relationship between them. Such chiral LEED patterns have been observed and reported on a number of naturally chiral, high Miller index Ag, Pt, and Cu surfaces.[6,8,29−34] The observation of LEED patterns from adsorbate layers on high Miller index surfaces is fairly rare, in part because there has been fairly little study of molecular adsorbates on high Miller index surfaces.[32,34] Although we have used LEED to look for the formation of ordered overlayers of TA on all of the surfaces used in this study, the only surfaces on which long-range order has been observed are $Cu(17,5,1)^{R\&S}$. In the case of TA on the $Cu(17,5,1)^{R\&S}$ surfaces, the LEED pattern from R,R-TA/$Cu(17,5,1)^R$ is equivalent but enantiomorphous to that from S,S-TA/$Cu(17,5,1)^S$. However, these differ from the LEED patterns obtained from S,S-TA/ $Cu(17,5,1)^R$ and R,R-TA/$Cu(17,5,1)^S$, which are also equivalent and enantiomorphous to one another. Thus, the ordered lattices of R,R- and S,S-TA on the $Cu(17,5,1)^{R\&S}$ surfaces exhibit structural diastereomerism, another indicator of enantiospecific adsorption.

The left-hand panel of Figure 3 reveals the decomposition kinetics of R,R- and S,S-TA on the $Cu(17,5,1)^{R\&S}$ surfaces. The structure of $Cu(17,5,1)$ differs from that of $Cu(643)$ in that the terrace, step, and kink of $Cu(17,5,1)$ are formed from the (100), (110), and (111) microfacets, respectively. The TA decomposition kinetics are highly enantiospecific, reaching a maximum of $r_S^{RR}/r_S^{SS} = r_R^{SS}/r_R^{RR} = 14$. Equally importantly, Figure

3 shows that the reaction kinetics exhibit true diastereomerism, $T_p^{RR/S} = T_p^{SS/R} < T_p^{RR/R} = T_p^{SS/S}$, proving that the origin of the differences lies in the relative handedness of the TA and the Cu surfaces. The right-hand panel of Figure 3 shows similar data for R,R- and S,S-TA on the $Cu(531)^{R\&S}$ surfaces. The $Cu(531)^{R\&S}$ surfaces are the "most chiral" fcc crystal surfaces in that they have the highest possible kink density. The TA decomposition kinetics on the $Cu(531)^{R\&S}$ surfaces are highly enantiospecific and exhibit true diastereomerism. It is important to note, however, that the order of stability of R,R- and S,S-TA on the $Cu(531)^{R\&S}$ surfaces is opposite to that on the $Cu(17,5,1)^{R\&S}$ surfaces: on $Cu(531)^{R\&S}$, $T_p^{RR/S} = T_p^{SS/R} > T_p^{RR/R} = T_p^{SS/S}$ and $r_S^{SS}/r_S^{RR} = r_R^{RR}/r_R^{SS} = 17$.

Decomposition of racemic TA on the chiral Cu surfaces ought to give one of two possible outcomes. If rac-TA separates into large homochiral domains, then a temperature pro- grammed reaction ought to reveal two resolved CO_2 desorption peaks, one for each of the two enantiomers. Although some chiral molecules separate into enantiomerically pure domains during adsorption, rac-TA on the $Cu(110)$ surface forms a racemate phase.[26] If a racemate is formed on a chiral surface, decomposition might be expected to occur at the lower of the two decomposition temperatures as the less stable enantiomer decomposes to form vacancies and the autocatalytic explosion then results in rapid decomposition of both enantiomers. Figure 3 shows the results of experiments in which $Cu(17,5,1)^{R\&S}$ and $Cu(531)^{R\&S}$ have been exposed to rac-TA. On $Cu(17,5,1)^{R\&S}$ the decomposition of the adsorbed rac-TA occurs at the lower of the two decomposition temperatures observed for the enantiomerically pure TA: $T_p^{rac/S} = T_p^{rac/R} = T_p^{SS/R} = T_p^{RR/S}$. The fact that $T_p^{rac/S} = T_p^{rac/R}$ is a consequence of the fact that rac-TA is achiral. In contrast to $Cu(17,5,1)^{R\&S}$, rac- TA on $Cu(531)^{R\&S}$ decomposes at the same temperature as the more stable of the pure enantiomers: $T_p^{rac/S} = T_p^{rac/R} = T_p^{RR/S} = T_p^{SS/R}$. Our interpretation of this result is that exposure of the chiral Cu surfaces to rac-TA in the gas phase does not result in

the adsorption of a racemic mixture on the surface. Because the surfaces are chiral, one of the two enantiomers will be preferentially adsorbed from the gas phase, yielding an enantiomerically enriched adsorbed layer; in this case, enriched in R,R-TA on $Cu(531)^S$ and in S,S-TA on $Cu(531)^R$. Unfortunately, there is no means of verifying this using TA because we have no experimental means of distinguishing R,R-TA from S,S-TA and determining their relative coverages once they are adsorbed on the surface. However, a similar experiment has been conducted using $Cu(3,1,17)^{R\&S}$ exposed to racemic aspartic acid (Asp, $HO_2CCH(NH_2)CH_2CO_2H$) in which the L-Asp enantiomer has been labeled with ^{13}C, thus allowing us to distinguish the decomposition products of D- and L-Asp using a mass spectrometer. As is expected for adsorption of rac-TA on $Cu(643)^{R\&S}$, rac-Asp exhibits enantiomeric enrichment on the surface following exposure to chiral $Cu(3,1,17)^{R\&S}$ surfaces.[16]

Another signature feature of the surface explosion reaction is that under isothermal conditions, the rate accelerates with extent of reaction. This is illustrated in Figure 4, which shows the decomposition rates as functions of time for R,R- and S,S-TA on $Cu(651)^S$ at constant temperatures in the range of 450−470 K. In all cases, there is an induction period during which there is no observable desorption of CO_2. During the induction period, a slow initiation process reduces θ^{TA} until the explosive, autocatalytic decomposition step begins to dominate and rapid acceleration of the reaction depletes the adsorbed TA. Isothermal decomposition also reveals extremely high enantio-selectivity; at 450 K, the enantiospecific ratio of the TA decomposition rates on $Cu(651)^S$ reaches $r_S^{RR}/r_S^{SS} = 12$.

DISCUSSION

The key point of this work is that the nonlinear nature of the surface explosion kinetics imparts extremely high enantiose-lectivity to reactions of chiral molecules on naturally chiral surfaces. In fact, our choice to study TA decomposition on naturally chiral surfaces was based on the fact that TA decomposition on $Cu(110)$ was known to occur via a vacancy mediated explosion mechanism which resulted in decom-position proceeding to completion over very narrow temper-ature ranges.[7,25,26] Our hypothesis was that this ought to lead to extremely enantiospecific reaction kinetics, as verified by this work. A recent and detailed study of the surface reaction kinetics for the explosive decomposition of TA/$Cu(110)$ has shown that they are well-described by a rate expression of the form

$$r = k_i\theta^{TA} + k_e\theta^{TA}(1 - \theta^{TA})^2 \qquad (1)$$

where the first term describes a first-order initiation process and the second term describes the explosive decomposition which is second-order in vacancy concentration.[7]

The rate expression of eq 1 has been used to extract the enantiospecific differences in the reaction energetics for R,R-TA and S,S-TA decomposition on the $Cu(651)^S$ surface from the isothermal decomposition rates illustrated in Figure 4. The peak reaction times under isothermal conditions can be used to define an effective rate constant at each temperature, $k_{eff} = t_p^{-1}$. These yield an enantiospecific ratio of the effective rate constants of $k_{eff}^{RR/S}/k_{eff}^{SS/S} = 1.34 \pm 0.13$ which yields a difference in the free energies of activation of $\Delta\Delta A_{SS/S}^{RR/S} = \Delta A^{RR/S} - \Delta A^{SS/S}$ $= 1.1 \pm 0.3$ kJ/mol. To first order, the rate law for vacancy-mediated explosion (eq 1) implies that $k_{eff} = (1/2)(k_ik_e)^{1/2}$

(see Supporting Information section). The lower right panel of Figure 4 plots $\ln(k_{eff})$ versus T^{-1} to yield the effective barriers derived from the two rates constants, $\Delta E_{eff} = (1/2)(\Delta E_i + \Delta E_e)$. The enantiospecificity of the effective barriers, $\Delta\Delta E_{eff} = \Delta E_{eff}^{RR/S} - \Delta E_{eff}^{SS/S}$, as estimated from these data is not significantly different from zero. Despite this, the nonlinear nature of the explosive decomposition kinetics leads to highly enantiospecific reaction rates, $r_S^{RR}/r_S^{SS} = 12$ at 450 K, based on the weakly enantiospecific difference in the relative rate constants, $k_{eff}^{RR/S}/k_{eff}^{SS/S} = 1.34 \pm 0.13$.

CONCLUSIONS

We have observed that the explosive decomposition of R,R- and S,S-TA on several naturally chiral, $Cu(hkl)^{R\&S}$ single crystal surfaces can exhibit enantiospecificities in reaction rates that reach factors of ∼50. The decomposition mechanism involves autocatalytic generation of vacancies in the adsorbed layer of TA resulting in kinetics similar to those of a radical branching explosion. From a mechanistic perspective this is the first heterogeneous, enantiospecific surface analogue of the homogeneous Soai reaction.[4,5] Like the Soai reaction, it is an autocatalytic process in which a chiral vacancy catalyzes the formation of another vacancy of the same chirality and as a direct result leads to high enantiospecificity. It should be pointed out, however, that the analogy with the Soai reaction is incomplete in the sense that the chirality of the vacancy is dictated by the crystallographic orientation of the Cu surface rather than just the chirality of the catalytic vacancy. Nonetheless the reaction has the characteristics of autocatalytic processes that have been postulated to lead to biomolecular homochirality in life on Earth; processes with relatively small differences in reaction energetics that, nonetheless, lead to extremely high enantioselectivity. Furthermore, these insights have the potential to lead to the rational design of highly enantioselective heterogeneous processes on chiral surfaces.

ASSOCIATED CONTENT

Ⓢ Supporting Information
Tabular list of the orientations of the low Miller index microfacets forming the structures of the chiral Cu surfaces; derivation of the relationship between the time to reach the peak reaction rate, t_p, observed during isothermal explosive decomposition of TA on Cu and the elementary rate constants for the initiation and explosion steps, k_i and k_e, respectively. This material is available free of charge via the Internet at http://pubs.acs.org.

AUTHOR INFORMATION

Corresponding Author
gellman@cmu.edu
Notes
The authors declare no competing financial interest.

ACKNOWLEDGMENTS

REFERENCES

(1) Bonner, W. A. *Origins Life Evol. Biospheres* **1991**, *21*, 59.

(2) Hazen, R. M.; Filley, T. R.; Goodfriend, G. A. *Proc. Natl. Acad. Sci. U.S.A.* **2001**, *98*, 5487.

(3) Hazen, R. M.; Sholl, D. S. *Nat. Mater.* **2003**, *2*, 367.

(4) Shibata, T.; Morioka, H.; Hayase, T.; Choji, K.; Soai, K. *J. Am. Chem. Soc.* **1996**, *118*, 471.

(5) Soai, K.; Osanai, S.; Kadowaki, K.; Yonekubo, S.; Shibata, T.; Sato, I. *J. Am. Chem. Soc.* **1999**, *121*, 11235.

(6) Rampulla, D. M.; Francis, A. J.; Knight, K. S.; Gellman, A. J. *J. Phys. Chem. B* **2006**, *110*, 10411.

(7) Mhatre, B. S.; Pushkarev, V. V.; Holsclaw, B.; Lawton, T. J.; Sykes, E. C. H.; Gellman, A. J. *J. Phys. Chem. C* **2013**.

(8) McFadden, C. F.; Cremer, P. S.; Gellman, A. J. *Langmuir* **1996**, *12*, 2483.

(9) Pratt, S. J.; Jenkins, S. J.; King, D. A. *Surf. Sci.* **2005**, *585*, L159.

(10) Ahmadi, A.; Attard, G.; Feliu, J.; Rodes, A. *Langmuir* **1999**, *15*, 2420.

(11) Sholl, D. S.; Asthagiri, A.; Power, T. D. *J. Phys. Chem. B* **2001**, *105*, 4771.

(12) Baber, A. E.; Gellman, A. J.; Sholl, D. S.; Sykes, E. C. H. *J. Phys. Chem. C* **2008**, *112*, 11086.

(13) Clegg, M. L.; Driver, S. M.; Blanco-Rey, M.; King, D. A. *J. Phys. Chem. C* **2010**, *114*, 4114.

(14) Horvath, J. D.; Gellman, A. J. *J. Am. Chem. Soc.* **2002**, *124*, 2384.

(15) Horvath, J. D.; Koritnik, A.; Kamakoti, P.; Sholl, D. S.; Gellman, A. J. *J. Am. Chem. Soc.* **2004**, *126*, 14988.

(16) Yun, Y.; Gellman, A. J. *Angew. Chem., Int. Ed.* **2013**, *52*, 1.

(17) Gellman, A. J.; Horvath, J. D.; Buelow, M. T. *J. Mol. Catal. A* **2001**, *167*, 3.

(18) Horvath, J. D.; Gellman, A. J. *J. Am. Chem. Soc.* **2001**, *123*, 7953.

(19) Rampulla, D. M.; Gellman, A. J. *Surf. Sci.* **2006**, *600*, 2823.

(20) Fleming, C.; King, M.; Kadodwala, M. *J. Phys. Chem. C* **2008**, *112*, 18299.

(21) Huang, Y.; Gellman, A. J. *Catal. Lett.* **2008**, *125*, 177.

(22) Cheong, W. Y.; Gellman, A. J. *J. Phys. Chem. C* **2011**, *115*, 1031.

(23) Pasteur, J. L. *Ann. Chim. Phys.* **1848**, *24*, 442.

(24) Lorenzo, M. O.; Baddeley, C. J.; Muryn, C.; Raval, R. *Nature* **2000**, *404*, 376.

(25) Lorenzo, M. O.; Humblot, V.; Murray, P.; Baddeley, C. J.; Haq, S.; Raval, R. *J. Catal.* **2002**, *205*, 123.

(26) Behzadi, B.; Romer, S.; Fasel, R.; Ernst, K. H. *J. Am. Chem. Soc.* **2004**, *126*, 9176.

(27) Falconer, J. L.; Madix, R. J. *Surf. Sci.* **1974**, *46*, 473.

(28) Sharpe, R. G.; Bowker, M. *J. Phys.: Condens. Matter* **1995**, *7*, 6379.

(29) Attard, G. A.; Ahmadi, A.; Feliu, J.; Rodes, A.; Herrero, E.; Blais, S.; Jerkiewicz, G. *J. Phys. Chem. B* **1999**, *103*, 1381.

(30) Puisto, S. R.; Held, G.; Ranea, V.; Jenkins, S. J.; Mola, E. E.; King, A. A. *J. Phys. Chem. B* **2005**, *109*, 22456.

(31) Francis, A. J.; Koritnik, A. J.; Gellman, A.; Salvador, P. A. *Surf. Sci.* **2007**, *601*, 1930.

(32) Gladys, M. J.; Stevens, A. V.; Scott, N. R.; Jones, G.; Batchelor, D.; Held, G. *J. Phys. Chem. C* **2007**, *111*, 8331.

(33) Jones, G.; Gladys, M. J.; Ottal, J.; Jenkins, S. J.; Held, G. *Phys. Rev. B* **2009**, *79*.

(34) Thomsen, L.; Tadich, A.; Riley, D. P.; Cowie, B. C. C.; Gladys, M. J. *J. Phys. Chem. C* **2012**, *116*, 9472.